Protoplasma (2006) 227: 165–173
DOI 10.1007/s00709-005-0141-3

PROTOPLASMA
Printed in Austria

Structural and immunocytochemical characterization of the *Ginkgo biloba* L. sperm motility apparatus

K. C. Vaughn[1,*] and **K. S. Renzaglia**[2]

[1] Southern Weed Science Research Unit, USDA Agricultural Research Service, Stoneville, Mississippi
[2] Department of Plant Biology, Southern Illinois University, Carbondale, Illinois

Received March 8, 2005; accepted June 3, 2005; published online May 30, 2006

Summary. *Ginkgo biloba* and the cycads are the only extant seed plants with motile sperm cells. However, there has been no immunocytochemical characterization of these gametes to determine if they share characteristics with the flagellated sperm found in bryophytes and pteridophytes or might give clues as to the relationships to nonflagellated sperm in all other seed plants. To determine characteristics of proteins associated with the motility apparatus in these motile sperm, we probed thin sections of developing spermatogenous cells of *Ginkgo biloba* with antibodies to acetylated and tyrosinated tubulin and monoclonal antibodies that recognize mammalian centrosomes and centrin. The blepharoplast that occurs as a precursor to the motility apparatus consists of an amorphous core, pitted with cavities containing microtubules and a surface studded with probasal bodies. The probasal bodies and microtubules within the blepharoplast cavities are labeled with antibodies specific to acetylated tubulin. Positive but weak reactions of the blepharoplast core occur with the centrosome-reactive antibodies MPM-2 and C-9. Reactions to centrin antibodies are negative at this developmental stage. From this pre–motility apparatus structure, an assemblage of about 1000 flagella and associated structures arises as the precursor to the motility apparatus for the sperm. The flagellar apparatus consists of a three-layered multilayered structure that subtends a layer of spline microtubules, a zone of amorphous material similar to that in the blepharoplast, and the flagellar band. Centrin antibodies react strongly with the multilayered structure, the transition zone of the flagella, and fibrillar material near the flagellar base at the surface of the amorphous material. Both the spline microtubules and all of the tubules in the flagella react strongly with the antibodies to acetylated tubulin. These localizations are consistent with the localizations of these components in pteridophyte and bryophyte spermatogenous cells, although the blepharoplast material surrounding and connecting flagellar bases does not occur in the seedless (nonseed) land plants. These data indicate that despite the large size of ginkgo gametes and the taxonomic separation between pteridophytes and *Ginkgo biloba*, similar proteins in gametes of both groups perform similar functions and are therefore homologous among these plants. Moreover, the presence of acetylated tubulin in bands of microtubules may be a characteristic shared with more derived nonflagellated sperm of other conifers and angiosperms.

Keywords: Centrin; Acetylated tubulin; Spermatogenous cell; Land plant evolution.

Introduction

Ginkgo biloba L. has been described as a living fossil, being the one extant species of a former large cosmopolitan group of plants. Although *Ginkgo biloba* is a gymnosperm, there are many unique aspects of this plant, one of the foremost being the mode of reproduction. Among seed plants, only ginkgo and cycads produce motile sperm cells (Renzaglia and Garbary 2001). These gametes are of particular interest because they are produced within a male gametophyte that is relatively long-lived (>4 months), is produced from pollen, and completes development within the ovule; the nucellus provides a substrate and nutrients required for male gametophyte maturation and the production of typically two sperm cells (Friedman 1987). Moreover, unlike male gametes of bryophytes and pteridophytes, which are relatively small (3–10 μm) and possess 2–150 flagella, sperm cells of ginkgo and cycads are relatively large (55–500 μm) and are equipped with 1000–50,000 flagella (Southworth and Cresti 1997, Renzaglia and Garbary 2001).

Hirase (1896) was able to observe the ellipsoidal shape and coiled anterior band of gingko sperm flagella as early as 1896. Unfortunately, these are difficult cells to study

* Correspondence and reprints: Southern Weed Science Research Unit, USDA Agricultural Research Service, P.O. Box 350, Stoneville, MS 38776, U.S.A.

because they develop rapidly after male gametophytes are mature and they are extremely short-lived. Friedman (1987) analyzed the development of the male gametophyte within the ovule and used three-dimensional (3-D) reconstruction to reveal its complex nature. After germination of the pollen grain, the male gametophyte grows for a period diffusely and then initiates tip growth, accompanied by a high degree of branching. Presumably at these stages, the male gametophyte uses the nucellar material of the megasporangium as nutritive tissue. Shortly before fertilization, the male gametophyte forms a saccate structure opposite the branched pollen tube, where the sperm cells differentiate (Gifford and Lin 1975, Friedman 1987).

In the central and southern United States, the pollination occurs in late March through April but the actual maturation of the sperm cells and fertilization does not take place until late August or early September (Friedman 1987; Renzaglia and Vaughn unpubl. obs.). Male gametes are present generally only a few days each year and these cells occur in a very protected region of the megasporangium in an area known as the fertilization chamber, at the apex of the female gametophyte (Friedman 1987). Because of the difficulty in finding these cells within the microgametophyte or free within the ovule and their limited duration, it is not surprising that only a few studies have been published on their ultrastructure (Gifford and Lin 1975, Gifford and Larson 1980, Li et al. 1989).

In this study we report the first results of immunocytochemical localizations of cytoskeletal proteins in the developing and mature flagellar apparatus of the gingko sperm. After similar studies on the less complex flagellar apparatus of pteridophytes and bryophytes (Hoffman et al. 1993, Vaughn and Harper 1998, Renzaglia and Vaughn 2000), it was of interest to determine what proteins and structures are shared and what either of these tells us about microtubule nucleation and organization in land plant sperm (Southworth and Cresti 1997).

Material and methods

Plant material

Ovules of *Ginkgo biloba* were collected from megasporangiate trees growing in Leland, Miss., and Carbondale, Ill., at the end of August and in early September at each location. Only certain days in each year at each site were male gametophytes at the appropriate stage for harvest.

Fixation and embedding

Micropylar tips of ovules, including a small apical portion of the female gametophyte with archegonia, covered by the nucellus, and the stony inner and fleshy outer integuments, were dissected with a razor blade. Integuments were separated and discarded and the nucellus was gently peeled off the female gametophyte with tweezers. Nucellar strips were then examined on their concave surfaces (facing the female gametophyte) for the presence of saccate male gametophytes. The samples were fixed in 3% glutaraldehyde in 0.05 M piperazine-N,N′-bis(2-ethanesulfonic acid) buffer (pH 7.4) and incubated in this fixative for 2 h at room temperature. After several buffer rinses, the tissues were dehydrated in ethanol and embedded in London Resin White resin slowly at 4 to −20 °C. The tissues were then agitated on a shaker for 24 h in 100% plastic. Samples were transferred to BEEM capsules and the resins cured at 50 °C in a vacuum oven.

Sectioning and section processing

Thick sections were cut with a Delaware HistoKnife at 0.35 to 0.50 μm and stained with toluidine so that the presence of the male gametophytes could be determined by light microscopy. When such tissues were encountered, the block was transferred to a Delaware diamond knife and sections were cut at about 100 nm (pale gold reflectance) and transferred to 300-mesh gold grids.

For immunogold labeling the grids were floated specimen side down on 4 μl drops of the following reagents for the indicated times: 1% bovine serum albumin (BSA) in phosphate-buffered saline (PBS), 30 min; primary antibody diluted 1 : 10 (acetylated tubulin, Sigma), 1 : 40 (tyrosinated tubulin, Sigma), 1 : 20 (MPM-2, gift of P. Rao), 1 : 40 (C-9, gift of J. Hoffman), 1 : 80, a polyclonal antibody raised to sea urchin tubulin (Polysciences, Warrington, Pa.), or 1 : 80 (centrin, gift of J. Salisbury) in PBS-BSA, 4 h; 4 drops of PBS-BSA, 2 min each; goat anti-mouse immunoglobulin G coupled to 15 nm diameter gold (for the monoclonals) or Protein A coupled to 15 nm diameter gold (for centrin polyclonal serum and sea urchin tubulin polyclonal serum), 30 min; 4 drops of PBS, 2 min each. Sea urchin anti-tubulin was only used on the blepharoplast stage spermatogenous cells. Controls consisted of the substitution of heat-denatured primary antibody at the same dilution as the nondenatured or no primary antibody. The grids were washed with double distilled water, dried, and poststained with 2% uranyl acetate for 2 min and lead citrate for 30 s prior to observation in a Zeiss EM 10 CR electron microscope. Low-magnification overview micrographs were taken using the "reduced-magnification" mode of this microscope that allows large areas of structure to be observed essentially at the level of the light microscope. Twenty micrographs from each of the localizations were used for quantification of immunogold labeling after being photographically enlarged to a magnification of ×60,000. Background label was calculated by counting gold particles from areas of cell wall in the same section. Values of zero immunogold label are given when the amount of label over a certain structure is equal to or less than background label by secondary antibody alone. For determination of the label, the number of gold particles per square micrometer of the area of blepharoplasts, flagella, basal bodies, or the multilayered structure was determined. Density of label on microtubules was determined as the number of gold particles per micrometer of the length of microtubules.

Comments on antibodies

Most of the antibodies used in this report have been used in numerous plant and animal systems and are well characterized. The C-9 antibody was raised to centrosomal extracts in a manner similar to that the MPM-2 antibodies were raised, but the C-9 antibody recognizes a nonphosphorylated centrosomal epitope.

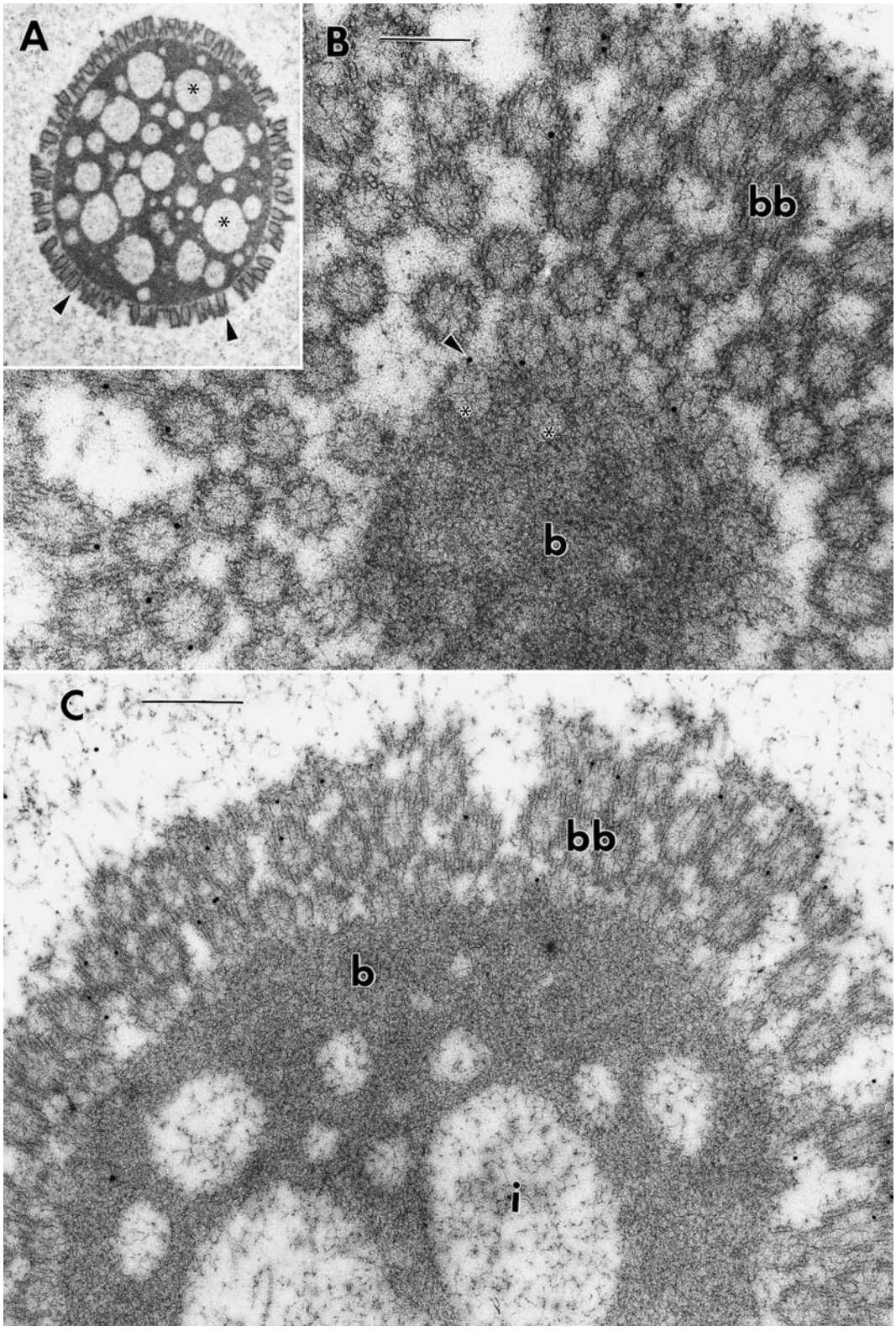

Fig. 1 A–C. *Ginkgo biloba* spermatogenous cells at the blepharoplast stage of development. **A** Reduced-magnification transmission electron micrograph of the blepharoplast. A central amorphous matrix is pitted with cavities or inclusion (asterisk) and surrounded by probasal bodies (arrowheads). **B** A section probed with anti-acetylated tubulin labels the probasal bodies (*bb*) but does not label the blepharoplast (*b*). Asterisks mark two structures on the blepharoplast surface that may be probasal body templates. **C** Anti-tyrosinated tubulin labels the probasal bodies (*bb*) but not the blepharoplast (*b*). *i* Inclusion or cavity. A, ×2000. Bar: B, 0.2 μm; C, 0.5 μm

Results

Blepharoplast stage

Two large (ca. 10 μm in diameter) spherical blepharoplasts form in each spermatogenous cell. The ground material of the blepharoplast is amorphous, gray granular material and is pitted by cavities that contain microtubules and occasionally basal bodies (Fig. 1A) (Renzaglia and Garbary 2002). The surface is studded with cylindrical probasal bodies that are oriented with their proximal end facing the outer surface of the blepharoplast. The probasal bodies are labeled with antibodies that recognize both acetylated (Fig. 1B) and tyrosinated tubulin (Fig. 1C). However, the matrix of the blepharoplast is not labeled by any of the tubulin antibodies (Figs. 1A, B and 2B and Table 1), including a polyclonal anti-sea urchin tubulin that recognizes a majority of the plant tubulins. Anti-centrin reactivity with the blepharoplast stage is not above background level of labeling in any of these structures (Fig. 2A and Table 1). The two monoclonal antibodies that recognize mammalian centrosomes, MPM-2 and C-9, both label the blepharoplast but labeling with either antibody is relatively low (Fig. 2C and Table 1). The microtubules present within the cavities within the blepharoplast are also labeled with the acetylated-tubulin monoclonal (Fig. 2D), as well as with all other tubulin antibodies (Table 1).

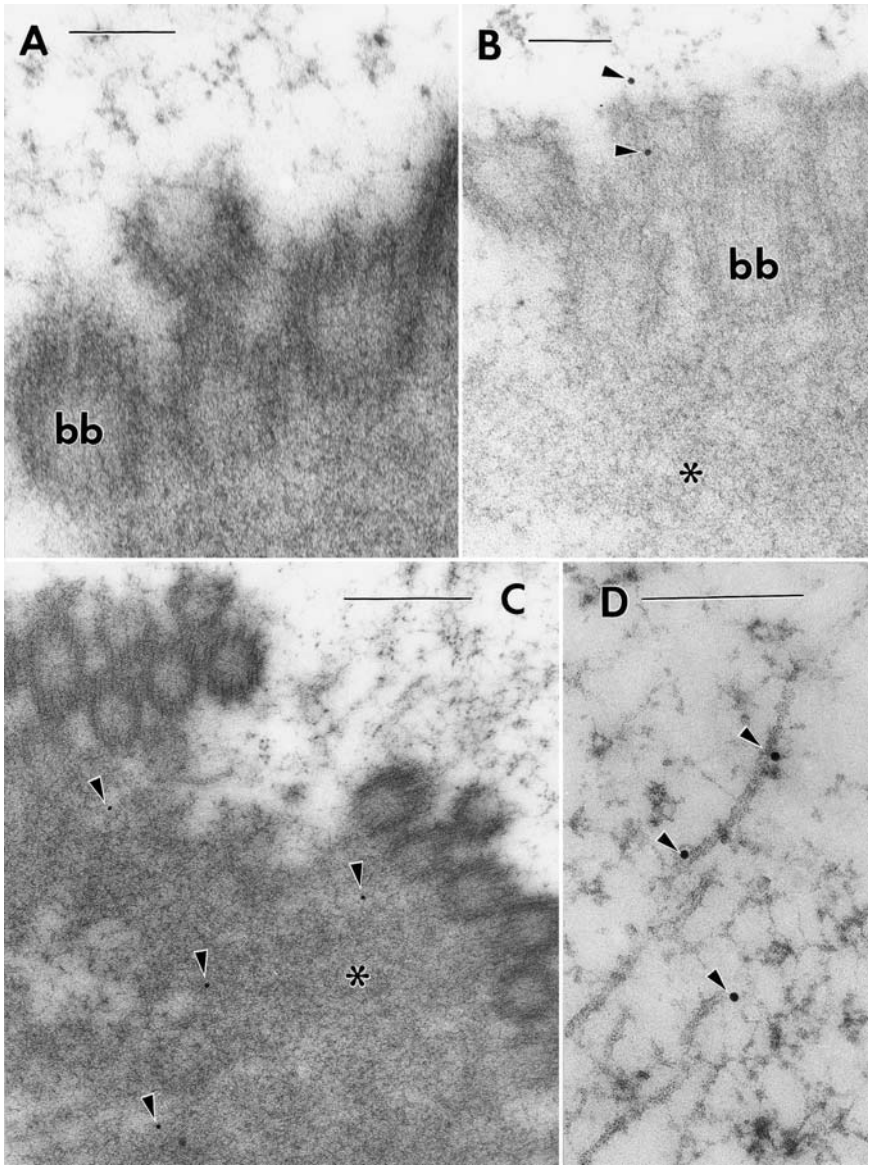

Fig. 2. Immunolocalizations of centrin (**A**), acetylated tubulin (**B** and **D**) and C-9 (**C**) in the blepharoplast stage. **A** No label is associated with either the probasal bodies (*bb*) or the blepharoplast matrix. **B** Acetylated-tubulin antibodies label the probasal bodies (*bb*) and microtubules associated with the growing end of a probasal body (arrowheads). **C** Sparse label in the blepharoplast gray granular material (asterisk) after labeling with the C-9 monoclonal that recognizes mammalian centrosomes (arrowheads). **D** Acetylated-tubulin antibodies recognize the microtubules present in the cavities of the blepharoplast. Arrowheads mark positive reactions. Bar: A, B, and D, 0.3 μm; C, 0.5 μm

Table 1. Immunogold labeling densities for various structures and stages in *Gingko biloba* spermatogenous cells

Stage and structure	Antibody	Label density[a]
Blepharoplast stage		
Blepharoplast matrix	centrin	0.0
	MPM-2	11
	C-9	7.0
	acetylated tubulin	0.0
	tyrosinated tubulin	0.0
	sea urchin tubulin	0.0
Probasal bodies	centrin	0.0
	MPM-2	0.0
	C-9	0.0
	acetylated tubulin	6.2
	tyrosinated tubulin	17
	sea urchin tubulin	32
Microtubules in inclusion	acetylated tubulin	21
	tyrosinated tubulin	14
	sea urchin tubulin	27
	all others	0.0
Mid-stage		
Lamellar strip	centrin	146
	all others	0.0
Spline	centrin	3.5
	acetylated tubulin	45
	tyrosinated tubulin	19
	all others	0.0
Blepharoplast remnants	centrin	1.2
	MPM-2	0.0
	C-9	1.4
	acetylated tubulin	1.2
	tyrosinated tubulin	0.0
Fibrillar material (not including blepharoplast remnants)	centrin	127
	all others	0.0
Flagella from basal body to plasma membrane	centrin	63
	acetylated tubulin	52
	tyrosinated tubulin	39
	all others	0.0
Flagella regions distal to plasma membrane	centrin	3
	acetylated tubulin	71
	tyrosinated tubulin	45
	all others	0.0

[a] Label density is expressed as number of gold particles per square micrometer of that structure minus the background label for all structures except microtubules. For microtubules, data are expressed as number of gold particles per micrometer of microtubule

Developing motile apparatus

The developing motility apparatus of the ginkgo sperm consists of several distinct structures and domains as described in Li et al. (1989). To help orient the reader, this is a brief synopsis of those features. A multilayered structure, consisting of a 3-layered lamellar strip and overlying layer of spline microtubules, is subtended by a very elongate mitochondrion. Two fibrous structures, sometimes referred to as osmiophilic crests in other species, are observed towards the terminus of the multilayered structure. A layer of amorphous material similar in appearance to the matrix of the blepharoplast connects the flagellar bases and coats the spline microtubule layer. Fibrillar material is associated with the distal surface of this mass. The basal bodies extend from the lamellar strip into an extremely elongate transition zone with stellate pattern to the plasma membrane. The distal end of the stellate pattern terminates at the plasma membrane boundary and coincides with a collar of electron-opaque material around the flagellar shaft on the plasma membrane surface.

Centrin antibodies strongly label the lamellar strip (Fig. 3A, B), the stellate pattern of the transition zone (Fig. 4A, B and inset), and fibrillar material on the surface of the gray granular material at the flagella bases (Fig. 3A, B). In the case of the fibrillar material overlying the amorphous material, occasional localizations are found on which the fibers at the surface may be clearly discerned, with centrin antibodies labeling these structures as they approach the surface of the section (Fig. 3A, B). The gray granular material resembling the blepharoplast (and labeled "el" in the micrograps of Li et al. [1989] but otherwise not named) separating the spline from the basal bodies does not react with anti-centrin (Fig. 4A), indicating that this material is derived from the similarly centrin-negative blepharoplast matrix material. Striated structures (called fibrous structures in Li et al. [1989]) are found towards the terminus of the multilayered structure but are also not labeled, despite their similarity in structure to the lamellar strip (not shown). Anti-centrin label is found throughout the stellate pattern and label stops coincident with the collar of electron-opaque material at the plasma membrane–flagella junction.

Although it is difficult to compare densities over such structurally distinct components, the strongest label with anti-centrin appears over the lamellar strip, with the weakest over the fibrillar material associated with the flagellar bases (Table 1). These differences might reflect the amount of centrin present plus the presence of other proteins or perhaps different conformers or possibly forms of centrin present within each of these structures.

In contrast to the sparse label with the acetylated-tubulin antibodies of the probasal bodies surrounding the blepharoplast (Figs. 1B and 2B), all of the microtubules were strongly labeled with this monoclonal (Fig. 5), including the flagellum throughout its length (Fig. 5A) and the spline microtubules that underlie the band of basal bodies (Fig. 5B). When one compares the label of the acetylated-tubulin antibody on the probasal bodies with that of the

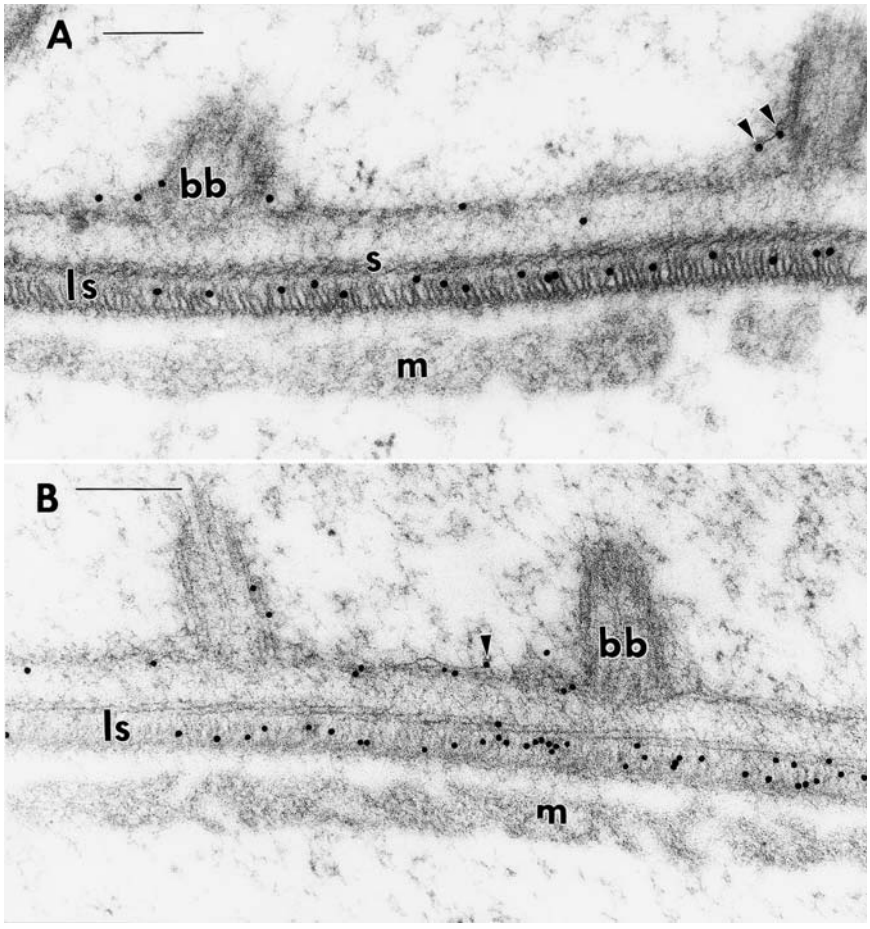

Fig. 3 A, B. Two views of the multilayered structure and associated basal bodies (*bb*) and anterior mitochondrion (*m*) in the sperm cells of ginkgo labeled with anti-centrin. Label is confined to the lamellar strip (*ls*) and a region of fibrils associated with the base of the basal bodies. Fibril ends are clearly labeled with anti-centrin. Bars: 0.2 μm

flagellum, there is about a 7-fold increase in label on a square micrometer basis (Table 1). In contrast, the amount of label on the microtubules in the spline layer is only approximately 2-fold on a linear micrometer basis to that found in the microtubules in the blepharoplast cavities (Table 1).

The only structure within the motility apparatus that is not labeled by centrin or any tubulin antibody is the amorphous, gray granular material that appears as a band separating the multilayered structure and flagella and into which the flagellar bases are inserted. Although we did observe weak label with the C-9 and MPM-2 antibodies at the blepharoplast stage (Fig. 2C and Table 1), we did not observe this label with blepharoplast remnants that coat the spline layer (not shown and Table 1). However, both of these antibodies label active centrosomes and microtubule-organizing centers (see Vaughn and Harper [1998] for a discussion) and the conversion of the blepharoplast might also involve a deactivation or proteolysis of those components of microtubule-organizing centers.

Discussion

Immunoreactivity of components of the gingko blepharoplast and motility apparatus and comparisons with pteridophytes

The motility apparatus of *Ginkgo biloba* sperm is one of the most elaborate in the plant kingdom, being bested only by the cycads in complexity and size (Norstog 1986). Despite this complex structure, the ginkgo blepharoplast and motility apparatus bears striking similarities to that of pterdidophytes, which have considerably fewer flagella than the 1000 present in ginkgo. As in the pteridophytes (Hoffman and Vaughn 1995), the blepharoplast serves as a basal body template and, although surrounded by tubulin-containing structures, contains no tubulin of its own but is reactive with anti-centrosomal antibodies such as MPM-2 and C-9. Similarly, although centrin is found in virtually all components of the motility apparatus in the pteridophytes (Vaughn et al. 1993) and ginkgo (this report), this

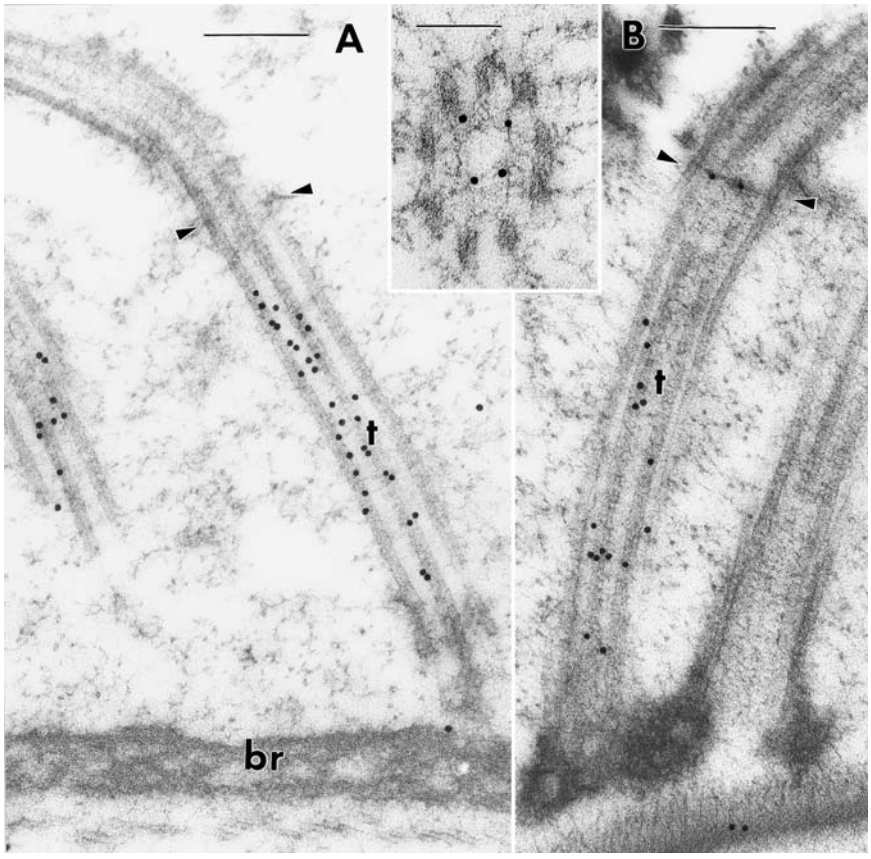

Fig. 4 A, B. Anti-centrin labeling of the transition zone in ginkgo sperm flagella. **A** Centrin label along the transition zone (*t*) but lack of label in the material near the flagellar bases that resembles a blepharoplast remnant (*br*). **B** Label in the transition zone extends all the way to an electron-opaque collar (arrowheads) but not past this structure. **Inset** Cross sectional view of the transition zone, showing the characteristic stellate pattern, labeled with anti-centrin. Bar: A and B, 0.3 μm; inset, 0.2 μm

protein is present at or below background levels in the blepharoplast and associated probasal bodies. Centrin is associated with the stellate pattern in the flagella. Thus, the absence of stellate pattern in these probasal bodies (e.g., Fig. 2A) is consistent with the lack of centrin reactivity. In the blepharoplast stage of gingko, spermatogenous cells contain the probasal bodies, whereas in pteridophytes, probasal bodies are not present until after the blepharoplast matrix has disintegrated. In many respects, the blepharoplast of gingko more resembles the "reorganizing blepharoplast" stage of the pteridophytes (Hoffman et al. 1994), in which only low levels of centrosomal antibody reactivity remains and probasal bodies are present.

In the motility apparatus, centrin label is associated with the multilayered structure, the stellate pattern of the transition zone, and small fibrils at the base of the flagellum (Figs. 3 and 4). Previous investigations of pteridophyte locomotory assemblages indicate a similar location of centrin in these structures (Vaughn et al. 1993, Hoffman and Vaughn 1995). Centrin is associated with the lamellar strip, amorphous zone, and transition zone of the flagellum in pteridophytes. However, the zone that would correspond to the amorphous zone in pteridophytes in ginkgo is composed mainly of the gray granular material similar to the blepharoplast interior and is unreactive to the centrin antibodies. Rather in ginkgo, only the fibrillar material at the surface of the structure seems to interact with flagellar bases. In this respect the centrin at the base of the flagellum in ginkgo compares more closely with centrin fibrils connecting the basal bodies in green algae (Melkonian et al. 1992, Vaughn and Harper 1998).

Comparisons of ginkgo sperm with that of land plants

Although the spermatogenous cells of *Ginkgo biloba* clearly resemble their pteridophyte ancestors in many ways, they might also give some clues as to the origin of structures present in angiosperm sperm cells. The most interesting similarity comes from the presence of acetylated tubulin in the sperm of both *Ginkgo biloba* and that of *Nicotiana tabacum* (Astrom 1992). Although angio-sperm spermatogenous cells do not possess flagella, micro-

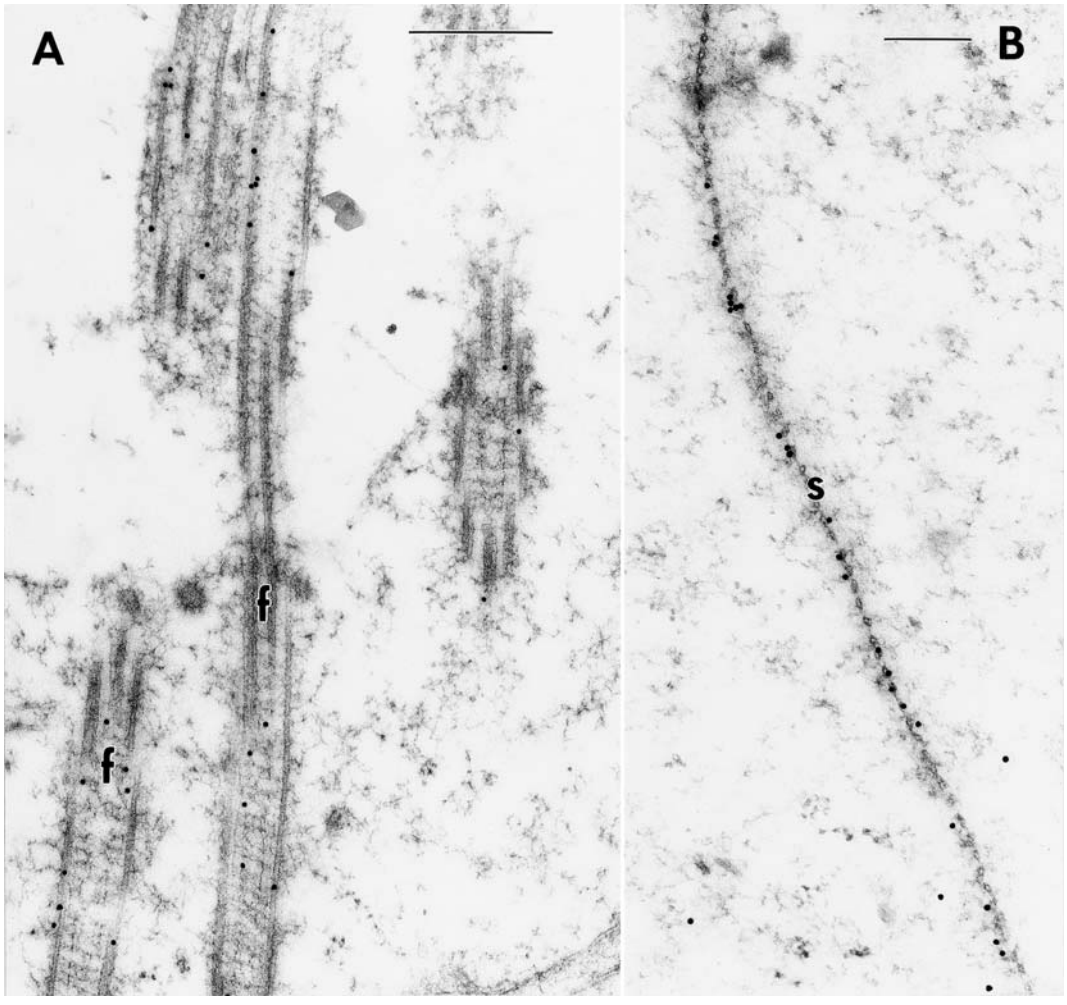

Fig. 5. Localization of acetylated tubulin flagella (**A**) and spline (**B**) microtubules. **A** Although centrin antibodies label the flagellum only through the transition zone, the acetylated-tubulin antibodies recognize the flagella (*f*) along their total length. **B** The spline microtubules (*s*) are strongly labeled with anti-acetylated tubulin antibodies. Bar: A, 0.5 μm; B, 0.3 μm

tubules often form bundles, not unlike the spline microtubule array (Palevitz and Tiezzi 1992, Southworth and Cresti 1997). This parallel is drawn further by the presence of the acetylated tubulin in these arrays, which in general is associated with more stable arrays (see review in Smertenko et al. [1997] and Gilmer et al. [1999]). In all sperm cells the microtubular bands may be utilized to alter nuclear shaping and it is possible this conserved function is a major reason why highly stabilized and cross-linked arrays of microtubules are requisite for a fully functional sperm cell. Previous work has shown that acetylated microtubule arrays are highly resistant even to microtubule disrupter herbicides (Hoffman and Vaughn 1995). Thus, it is obvious that the plant has gone to an extreme case to protect these microtubules through this very important function.

It is clear from this work that a comprehensive study should examine sperm of various species for the presence of microtubule arrays containing acetylated tubulin as this tubulin modification appears to be a key and unique factor in spermatogenous cells in all land plants. Moreover, the presence of acetylated microtubule arrays in other basal land plants might give clues as to the evolution of the spline into the similar microtubules in angiosperm sperm cells.

Acknowledgments

Thanks are extended to Brian Maxwell and Lynn Libous-Bailey for technical assistance and to Christopher Meloche for stimulating discussions. Two anonymous reviewers greatly improved the text. Thanks are extended to J. Salisbury, P. Rao, and J. Hoffman for some of the antibodies used in these studies. This work was supported by NSF grant DEB-9527735 to K.S.R. Mention of a trademark, brand, or proprietary product does not constitute an endorsement by the USDA.

References

Astrom H (1992) Acetylated alpha tubulin in the pollen tube microtubules. Cell Biol Int Rep 9: 208–219

Friedman WE (1987) Growth and development of the male gametophyte of *Ginkgo biloba* within the ovule (in vivo). Am J Bot 74: 1797–1815

Gifford EM, Lin J (1975) Light microscopic and ultrastructural studies of the male gametophyte in *Ginkgo biloba*: the spermatogenous cell. Am J Bot 62: 974–981

Gifford EM, Larson S (1980) Developmental features of the spermatogenous cell in *Ginkgo biloba*. Am J Bot 67: 119–124

Gilmer S, Clay P, MacRae TH, Fowke LC (1999) Acetylated tubulin is found in all microtubule arrays of two species of pine. Protoplasma 207: 174–185

Hirase S (1896) On the spermatazoid of *Gingko biloba* (in Japanese). Bot Mag (Tokyo) 10: 325–328

Hoffman JC, Vaughn KC (1995) Post-translational tubulin modification in spermatogenous cells of the pteridophyte *Ceratopteris richardii*. Protoplasma 186: 169–182

Hoffman JC, Vaughn KC, Joshi HC (1994) Structural and immunocytochemical characterization of microtubule organizing centers in pteridophyte spermatogenous cells. Protoplasma 179: 46–60

Li Y, Wang FH, Knox RB (1989) Ultrastructural analysis of the flagellar apparatus in sperm cells of *Ginkgo biloba*. Protoplasma 149: 57–63

Melkonian M, Beech PL, Katsaros C, Schulze D (1992) Centrin-mediated cell motility in algae. In: Melkonian M (ed) Algal cell motility. Chapman and Hall, New York, pp 179–221

Norstog K (1986) The blepharoplast of *Zamia pumila* L. Bot Gaz 147: 40–46

Palevitz BA, Tiezzi A (1992) The organization, composition and function of the generative cell and sperm cytoskeleton. Int Rev Cytol 140: 149–185

Renzaglia KS, Garbary DJ (2001) Motile gametes of land plants: diversity, development and evolution. Crit Rev Plant Sci 20: 107–213

Smertenko A, Blume Y, Vilicky V, Opartny Z, Draber P (1997) Post-translational modifications and multiple tubulin isoforms in *Nicotiana tabacum* L. cells. Planta 201: 349–358

Southworth D, Cresti M (1997) Comparisons of flagellated and nonflagellated sperm in plants. Am J Bot 84: 1301–1311

Vaughn KC, Harper JD (1998) Microtubule-organizing centers and nucleating sites in land plants. Int Rev Cytol 181: 75–149

Vaughn KC, Sherman TD, Renzaglia KS (1993) A centrin homologue is a component of the multilayered structure in bryophytes and pteridophytes. Protoplasma 175: 58–66